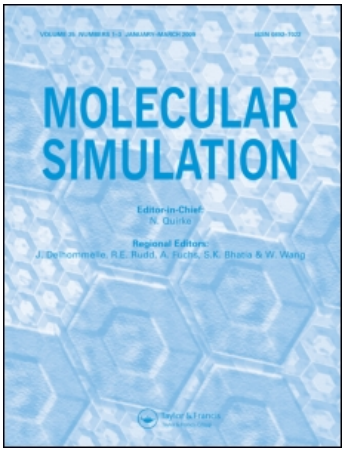

Molecular Simulation
Publication details, including instructions for authors and subscription information:
http://www.informaworld.com/smpp/title~content=t713644482

Temperature-quench Molecular Dynamics Simulations for Fluid Phase Equilibria

F. Martínez-Veracoechea[a]; E. A. Müller[b]
[a] Departamento de Termodinámica y Fenómenos de Transferencia, Universidad Simón Bolívar, Caracas, Venezuela [b] Department of Chemical Engineering and Chemical Technology, Imperial College, London, UK

To cite this Article Martínez-Veracoechea, F. and Müller, E. A.(2005) 'Temperature-quench Molecular Dynamics Simulations for Fluid Phase Equilibria', Molecular Simulation, 31: 1, 33 — 43
To link to this Article: DOI: 10.1080/08927020412331298991
URL: http://dx.doi.org/10.1080/08927020412331298991

Molecular Simulation, Vol. 31 (1), 15 January 2005, pp. 33–43

Taylor & Francis
Taylor & Francis Group

Temperature-quench Molecular Dynamics Simulations for Fluid Phase Equilibria

F. MARTÍNEZ-VERACOECHEA[a,*] and E.A. MÜLLER[b,†]

[a]*Departamento de Termodinámica y Fenómenos de Transferencia, Universidad Simón Bolívar, Caracas 1080, Venezuela;* [b]*Department of Chemical Engineering and Chemical Technology, Imperial College, London, SW7 2AZ, UK*

(Received July 2004; In final form July 2004)

A method for locating fluid phase equilibria by means of a single canonical molecular dynamics simulation is evaluated. The temperature-quench molecular dynamics (TQMD) method consists of quenching an initially homogeneous one-phase fluid system to a lower temperature where it is mechanically and thermodynamically unstable. After a short transient, domains of coexisting phases form, which quickly acquire equilibrium-like properties. A suitable analysis of the coexisting domains in terms of local densities, compositions, or some other order parameter gives the phase equilibrium properties. We show how, contrary to expectations, one need not wait until a full global equilibration (planar interface) is resolved to obtain the correct results. As examples, the phase diagram of a cut and shift (5σ) Lennard–Jones fluid, the pressure-composition diagram of a Lennard–Jones mixture presenting three-phase vapor–liquid–liquid equilibria and the saturated liquid densities of eicosane using a united atom representation are determined. Comments and comparisons are made with the most commonly used methods such as Gibbs Ensemble Monte Carlo and volume expansion molecular dynamics (VEMD), finding TQMD to be a suitable alternative, especially for complex molecules and/or high densities.

Keywords: Fluid phase equilibria; Vapor–liquid equilibrium; Vapor–liquid–liquid equilibria; Lennard–Jones; Eicosane

INTRODUCTION

The application of Molecular Dynamics (MD) simulations to the phase equilibria of fluids has a relatively long history [1]. In a typical implementation [2,3], previously equilibrated fractions of a bulk liquid and bulk vapor phase are placed in a single simulation box in the form of a slab of liquid surrounded by a vapor phase. The system is then allowed to evolve under canonical (constant density and temperature) conditions until equilibration is reached through diffusive mass transport. The simultaneous simulation of two bulk phases and the two corresponding interfaces, along with relatively slow diffusion, made these methods costly from a computational point of view. In this scenario, the development of the Gibbs Ensemble Monte Carlo (GEMC) [4] almost two decades ago, offered a substantial computational advantage since it allowed the modeling of fluid phase equilibria without the explicit inclusion of the interfacial region and since then has become the *de facto* simulation method for generating phase diagrams for fluid systems. However, the GEMC method is not without limitations [4], particularly, in the context of the simulation of very dense phases and/or complex molecules. Nowadays, mainly due to notable improvements in hardware available, MD algorithms may be easily implemented on parallel computers, decreasing sometimes by an order of magnitude of the simulation times of comparable serial runs. Also, MD is a natural choice for the simulation of dense phases and has the potential of being applicable to more complex systems than those that can be resolved via conventional MC methods. As a product of these observations, some recent papers have been published oriented towards modeling of phase equilibria using MD [5–9], although the emphasis has been on the determination of interfacial properties.

There is no unique methodology to perform phase equilibria calculations using MD. Typically, in the so-called "direct methods", systems with a

* Tel.: +58-212-9063740. Fax: +58-212-9063743. E-mail: emuller@usb.ve
†Corresponding author. Tel.: +44-20-75945557. Fax: +44-20-75945604. E-mail: e.a.muller@imperial.ac.uk

ISSN 0892-7022 print/ISSN 1029-0435 online © 2005 Taylor & Francis Ltd
DOI: 10.1080/08927020412331298991

previously equilibrated condensed phase are put into contact with either a corresponding vapor phase or vacuum. The system is then left to evolve under canonical conditions. Bulk regions separated by flat interfaces are set up from the onset and vary only due to diffusion. In a previous paper [10], we outlined a method that allows the location of phase coexistence through a constant density simulation in which the temperature of a homogeneous one-phase system is changed in a single time step (quenching) in such a way to place the system in a thermodynamically and mechanically unstable state. At this point the system spontaneously separates into domains of stable, locally equilibrated phases. Small clusters nucleate, which rapidly grow due to the strong driving force. The clusters will coalesce and eventually form macroscopic domains. Contrary to our assumption, phase coexistence data may be gathered from these locally equilibrated sub-domains, not being necessary to continue the simulation until global equilibrium is reached, resulting in a dramatic savings of computational effort. This temperature-quench molecular dynamics (TQMD) method showed promise in modeling phase equilibria of vapor–liquid, liquid–liquid and even solid–liquid equilibria [10,11]. This paper gives a more detailed account of the method and particularly analyzes the short-time phase separation behavior of fluids upon which it is based, as well as example applications to the vapor–liquid equilibria of a pure LJ fluid, the liquid–liquid–vapor equilibria of a binary LJ system, and the saturation densities of a long-chain alkane.

TEMPERATURE-QUENCH MOLECULAR DYNAMICS (TQMD)

Overview of the Method

Consider, for simplicity, a single-component liquid–vapor system. One starts out with a system composed of a given number of particles N, volume V and temperature T, large enough to guarantee a one-phase system. Keeping both N and V constant, the temperature, which is controlled by means of a "thermostat", is lowered abruptly. The new temperature must be such that the resulting state point lies within the spinodal envelope, e.g. at conditions that are both mechanically and thermodynamically unstable. As the system relaxes at the new state point, domains of liquid and vapor form on timescales easily accessible to molecular dynamics simulations. The connectivity and morphology of these phases will depend on their volume fractions. This spinodal decomposition process has been studied elsewhere [12–14], albeit not in the context of fluid phase equilibria. In Fig. 1, we present a sequence of snapshots that show a typical evolution. Immediately after quenching, the system is far from equilibrium and the driving force for diffusive transport is maximized (state a). At short times (states b and c) the surface area between the two phases is very large, and the combination of these two factors ensures that local densities and concentrations stabilize at their equilibrium values very quickly. It is at this point that, in the context of the TQMD method, statistics regarding concentrations and densities of coexisting phases may be obtained. At later times, the reduction of surface tension between the two phases is the driving force for the observed "coarsening". This latter evolution is comparatively slow. If enough time elapses, the system equilibrates to domains separated by flat interfaces (state d).

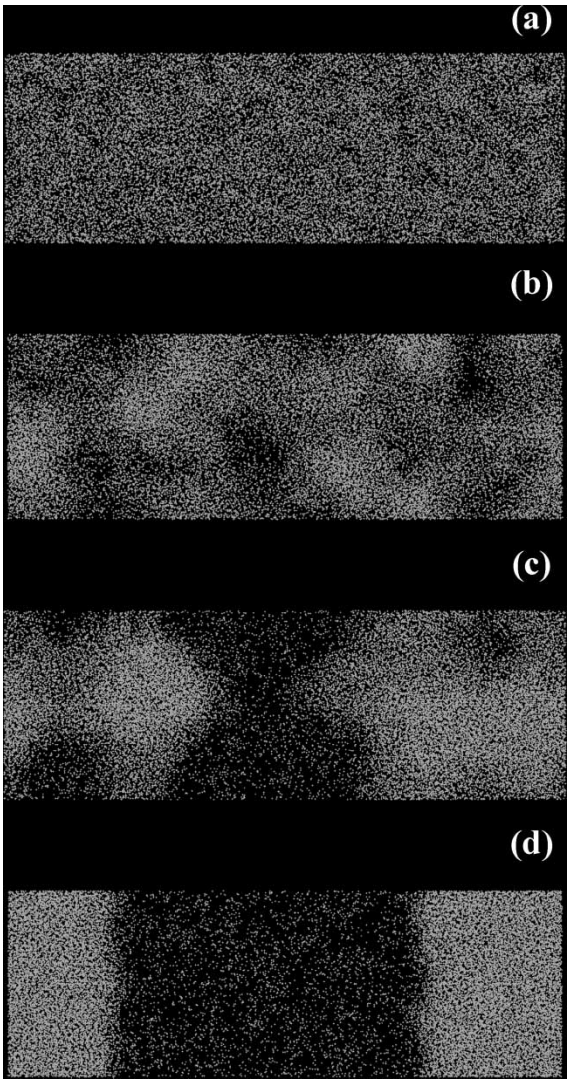

FIGURE 1 Snapshots of configurations of a system with 30,000 LJ particles after quenching to a temperature, $T^* = 1.1$. The system evolution after 1000, 15,000, 90,000 and 300,000 time steps, respectively, are shown in (a)–(d). From state point (c), it is possible to obtain accurate densities for both phases using the methods described here.

Interface Detection

To estimate the local equilibrium densities in a multiphase system we could wait until the system shows two distinct domains divided by flat interfaces. By choosing the simulation box in such a way that one of its axes is longer than the other two, at long simulation times (e.g. state d in Fig. 1) the planar interface will form normal to the longer axis. The density profile along such axis can be fitted to a smooth stepwise function, thus allowing for the calculation of the bulk densities and the profiling of the interface (see Ref. [9] for an example application). However, the evolution of the system into global equilibrium may be time consuming, even for today's computers and especially for larger systems and/or multicomponent systems. This paper strives to note that the equilibrium property analysis may be performed much before the system attains global equilibrium, thus decreasing the necessary computation time by more than half in most of the cases. If one stops the simulation at a point in which certain domains are formed, even if they are not consolidated, e.g. the insert in Fig. 2, one may divide the system into small subcells, and for each of these, determine the local density (and/or compositions and/or some suitable order parameter). The collection of this information in the form of frequency against a given density range (or composition or order parameter) gives a histogram which profiles the overall system. As an example, we show in Fig. 2 the results of the simulation of a liquid–vapor binary system described in detail in the "Results" section. The histogram shows two obvious peaks, corresponding to the vapor and liquid average densities. We shall further detail our observations on the analysis of such histograms.

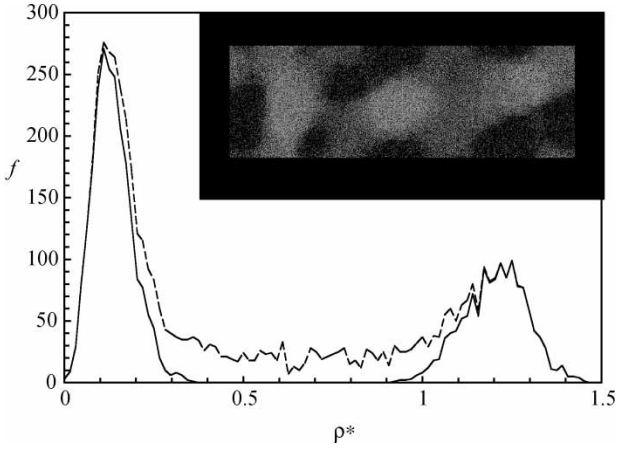

FIGURE 2 Frequency of occurrence, f, as a function of the subcell density ρ^* for a configuration of a binary system of 180,000 LJ particles, $T^* = 1$, overall composition $z_1 = 0.1$ after 100,000 time steps. Further system details are given in the "Results" section. Dashed line is the "raw" histogram; solid line is after interface removal. Sub-cell length, $L^* = 5$. The insert shows a snapshot of the system.

The choice of sub-cell size to perform the histogramming is not trivial. The sub-cells must be large enough that they can give a reasonable estimate of the density of a single phase; if the cells are too small, the density histogram will be "quantized" due to the small integer number of particles that can fit in each one. A sub-cell of volume V may only have densities of the form n/V with n being an integer, e.g. the possible densities for a cubic sub-cell with side 3σ (volume $27\sigma^3$) will be 0, 0.03704, 0.0741, 0.1111, etc. The larger the sub-cell size, the finer the density histogram, since the separation between the acceptable values of the histogram diminishes. However, since the system is analyzed before the phases cluster into single domains separated by planar interfaces, the interface is not clearly localized, but disperse between the clusters within the box. Thus, the use of large sub-domains will contribute to have a larger number of boxes that include significant portions of two (or more) phases. These sub-cells with a mixture of phases contribute to the "smearing out" of the histogram. The optimal sub-cell size, although an arbitrary quantity, is a compromise between these competing requirements.

Whichever division of the system is employed for the data analysis, some sub-cells will contain significant portions of two (or more) phases. We make a proposal for detecting and avoiding this situation based on a microscopic analysis of the fluid configuration, so as to only collect histogram data in sub-cells that contain entirely one phase. For example, if we choose the average coordination number as the proper order parameter, we can define an upper (CNU) and lower (CNL) bound coordination number for which a molecule is considered as a member of each phase. The coordination number is defined arbitrarily as the number of neighbors a molecule will have within a fixed radius. In this work we used a radius of $2\sigma_1$. Particles that are "in" an interface between two phases have coordination numbers reflecting the interfacial region; e.g. in the case of vapor–liquid equilibria, they have neighbors lesser than particles in the liquid phase, and greater than particles in the vapor phase. By counting the local coordination of every particle, these can be identified unambiguously. Sub-cells that contain more than 15% "interfacial" particles are then (arbitrarily) excluded from the histogram count. In the case of discrimination by mole-fraction, a similar algorithm can be applied to a single species; for every particle, one counts the total number of neighbors of a single species, and locates particles on the interface by values of this quantity that fall between those of the pure phases. For more complex systems other order parameters may be developed. In all cases it is necessary to have only a rough estimate of the density or concentration differences between the two phases, which is easily obtained through computer graphics

visualizations of the quenched system. It is important to note that this detection procedure and the data collection in this method does not affect the MD trajectory in any way, and can be done after the simulation has completed. Furthermore, the cost of this analysis is low, and can be easily repeated many times using different detection methods, interface definitions, percentage of tolerance (e.g. the amount of interfacial molecules allowed in sub-cell) etc. without increasing the total cost of the calculation.

As an example, in Fig. 2 we show the resulting "raw" histogram (dashed line), in which we plot the frequency of occurrence of a given density within each of the 10,125 subcells in which a given configuration is divided. Two peaks corresponding to the liquid and vapor phases are clearly visible, but there is considerable noise in the region between the peaks, which comes from the cells that contain many "interfacial" particles. In this case, the values of $\mathrm{CNL} = 12$ and $\mathrm{CNU} = 28$ are used. With these values, the cells containing more than 15% of interfacial particles (i.e. particles with a coordination number larger than CNL and smaller than CNU) are eliminated and one obtains a "clean" histogram as the one shown with a solid line in Fig. 2, and definitive values of the densities (vapor $\rho^*_{\mathrm{V}} = 0.135$ and liquid $\rho^*_{\mathrm{L}} = 1.214$) for this configuration.

The phase density determination by use of coordination numbers may be extended in the case of liquid–liquid equilibria if one takes into account coordination numbers based on particular components, e.g. a concept analogous to determining local compositions. In the case of ordered phases, such as the isotropic-nematic equilibria found in liquid crystals, other suitable order parameters can be used to discern between phases.

Calculation of compositions with TQMD might, in principle, be performed using composition histograms. However, the added degrees of freedom make it impractical. For multicomponent cases, upon deletion of the subcells containing interfacial molecules (on the basis for example of CN based on the presence of a particular component), one may discriminate the remaining subcells as belonging to either of the coexisting phases. The overall compositions are obtained by simple average of the compositions of all subcells forming part of that given phase. The extension to multiple phase equilibria is straightforward.

Determination of Equilibrium Properties

One may attempt to choose the maximum shown in the histograms to obtain the corresponding phase densities. However, such a procedure is quantitatively poor due to the quantization of the histogram, and thus the accuracy of the estimation will be of the order of magnitude of the bin size of the histograms.

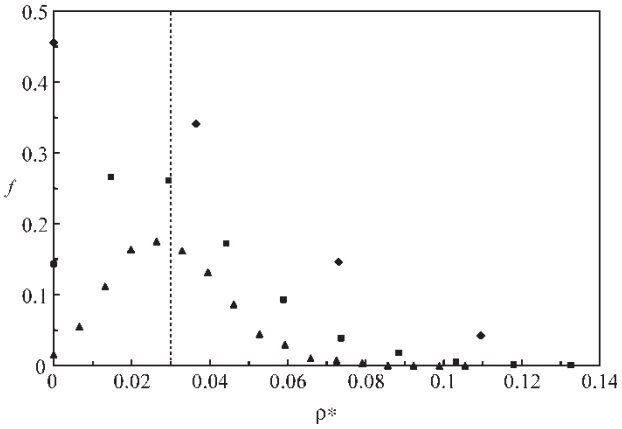

FIGURE 3 Frequency of occurrence, f, as a function of the subcell density ρ^* for a 5000 particle one-phase LJ fluid at an overall density of $\rho^* = 0.03$ and a temperature of $T^* = 1.1$. In each case, the subcell length, L^* used for collecting the histograms is varied; diamonds are $L^* = 3.0146$, squares are $L^* = 4.0786$, triangles are $L^* = 5.3335$. Dashed line corresponds to the overall density of $\rho^* = 0.03$.

To further illustrate this point, we describe here the analysis of a pure 5000 LJ particle one-phase vapor system with previously fixed density of $\rho^* = 0.03$ at $T^* = 1.1$. On an equilibrium configuration of this system we have determined the histogram distributions using three different sub-cell sizes. One might mention that even though the sub-cell size is arbitrary, if one wishes to include the total amount of information available, the side length of the sub-cells should be a discrete fraction of that of the global system. We have used cubic subcells with side length $L^* = 3.0146$, 4.0786 and 5.3335. It is seen from the resulting histograms in Fig. 3, that if one assumes that the maximum frequency of occurrence corresponds to the mean density, the results are erroneous (densities of 0, 0.01474 and 0.02636 would be obtained, respectively). However, in all cases, either a maximum likelihood analysis or a weighted average of the histograms will give the correct (0.03) result.

We point out that all these calculations are performed after the simulation has concluded, since they are analysis of the final configurations. An improvement of the statistics may be obtained by consolidating the information from several different configurations, separated by appropriate time steps. Otherwise, larger system sizes improve the statistics in a natural way, although consuming longer simulation times, as is shown in the results.

RESULTS AND DISCUSSION

The method described is general in nature and not limited in scope to any particular type of intermolecular potential. For the purpose of testing and comparing the method we will outline three typical

applications: (1) a simple pure fluid, for which the temperature–density phase diagram is sought. For this system GEMC would be the simulation method of choice; (2) a binary mixture, where there is a multiplicity of phase behaviors including three phase liquid–liquid–vapor; and (3) a long-chain alkane molecule, where particle-insertion methods would be difficult to implement.

Pure LJ CS Fluid

Simulations were carried out to determine the phase diagram of a pure Lennard–Jones fluid with a CS potential at a radius of $r_c = 5\,\sigma$. Results will be given in the usual LJ reduced units [15]. A total of 30,000 particles and 300,000 time steps were used to obtain the results at lower temperatures ($T^* < 1.2$) and 50,000 particles and 400,000 time steps for the highest one. The results are given in Table I, where they can be quantitatively compared to those obtained from GEMC runs on 4000 particle systems, discarding the initial 40×10^6 configurations and averaging over 100×10^6 configurations. All results compare well within statistical uncertainties. The lowest temperature point ($T^* = 0.7$) was not reported for GEMC, due to the poor statistics obtained caused by the failure of the particle insertion step to accurately sample the high density of the corresponding liquid. This deficiency may be circumvented with more advanced techniques [4], which are not the point of this paper. The critical temperature $T_c^* = 1.275 \pm 0.004$ and density $\rho_c^* = 0.319 \pm 0.003$ were estimated using the usual Ising scaling construction, (i.e. by the intersection of the rectilinear diameter of the coexistence curve with the scaled temperature–density relation using an Ising exponent of 0.32 [16]) applied to the TQMD data.

Since the systems studied contain an interface, one may not apply the virial theorem to obtain the pressure in a direct manner due to its ambiguous definition when an interface is present. A recent review [17] exemplifies the problems involved. In the case of an elongated box in which two phases are separated by a planar interface, the system pressure may be estimated by calculating the normal component of the pressure tensor. In practice, this works only on the vapor phase and requires the existence of a single planar interface. In TQMD, this final equilibrium state (planar interface) is not necessarily attained, and in fact is undesirable. After calculating the equilibrium densities, we performed a canonical MD simulation of a rather small (we used $N = 10^4$, although much smaller system sizes may be used for this purpose) homogeneous system with the specified temperature and density to obtain the pressure, by use of the virial theorem, of each coexisting phase. As it turns out, due to the low values of the compressibility of the dense phase, small errors in the density imply large errors in pressure. Thus, the pressures were obtained by using the vapor phase density, when available. The critical pressure $P_c^* = 0.120 \pm 0.004$ was estimated by extrapolation of the saturation curve to the critical density found above.

Figures 4 and 5 show the time evolution, in terms of MD time steps, of the vapor and the liquid densities respectively, for the runs made at $T^* = 1.1$. It is seen that TQMD converges rather rapidly to the expected (GEMC) equilibrium value, in spite of not having attained a flat interface. Note that the error bars on the GEMC result are large on the scale of the plot (± 0.006 and ± 0.02 for the vapor and liquid, respectively), and so the final quantitative agreement is excellent. While the results at $T^* = 1.1$ are typical of those obtained here, at lower temperatures the progress towards an equilibrium value is accelerated and at higher ones it is slowed down.

The results are compared to those obtained using a system of 500,000 particles. While agreeably, this system size is far larger that that needed for this particular application, it is the order of magnitude that is needed for studies of multicomponent mixtures, asymmetric and/or multiphase fluids. As expected, there is a noticeable improvement with respect to the stability of the approach towards the expected equilibrium values, e.g. the smaller system size shows greater fluctuations. It is interesting to note that in terms of the number of time steps

TABLE I Saturated vapor density, ρ_v^*, liquid density, ρ_l^*, and pressure P^* as a function of temperature T^* for a pure LJ cut and shifted ($r_c^* = 5$) potential as obtained from TQMD and GEMC

	TQMD			*GEMC*		
T^*	ρ_v^*	ρ_l^*	P^*	ρ_v^*	ρ_l^*	P^*
0.7	0.0023(3)	0.832(1)	0.0016(2)			
0.8	0.0071(4)	0.785(1)	0.0054(3)	0.0071(5)	0.79(1)	0.0054(4)
0.9	0.0173(5)	0.742(1)	0.0139(5)	0.016(2)	0.74(2)	0.013(1)
1	0.0332(5)	0.688(1)	0.0276(5)	0.034(2)	0.69(1)	0.028(2)
1.1	0.0655(2)	0.627(1)	0.0516(4)	0.063(6)	0.625(10)	0.051(5)
1.2	0.1206(8)	0.549(3)	0.086(1)	0.117(7)	0.54(1)	0.085(5)
1.275(4)	0.319(3)	0.319(3)	0.120(4)			

Critical point (last line) is estimated using the TQMD data. 0.123(4) corresponds to 0.123 ± 0.004.

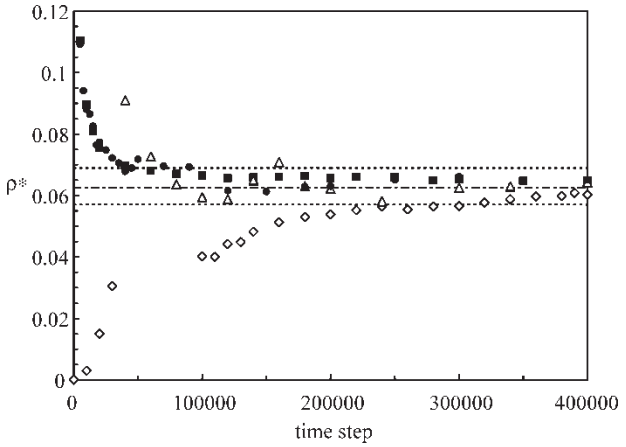

FIGURE 4 Vapor density ρ_V^* for a pure LJ fluid at a temperature of $T^* = 1.1$ as a function of the number of time steps. Solid symbols correspond to the results using TQMD; circles are for a system of 30,000 particles, squares are for a system of 500,000 particles. Open symbols correspond to the results using VEMD; triangles are for a system of 30,000 particles, diamonds are for a system of 500,000 particles. The dashed–dotted line is the GEMC value, dashed lines are the confidence intervals.

required to obtain a suitable density estimate, both the systems behave similarly; after roughly 100,000 time steps the density analysis gives the same resulting value. By increasing the system size we are including a larger statistical population and improving the statistics. This confirms the fact that the cluster size needed for the accurate determination of equilibrium properties is small.

Another interesting comment corresponds to the visual perception of the attainment of equilibrium. It is seen from the snapshots shown in Fig. 1 (which correspond to the small TQMD system referred to in Figs. 4 and 5), that at 90,000 time steps, the system is far from being considered at global equilibrium, however, the densities of the corresponding phases have already achieved their equilibrium values, as shown in Figs. 4 and 5. Figure 6 shows the short-time

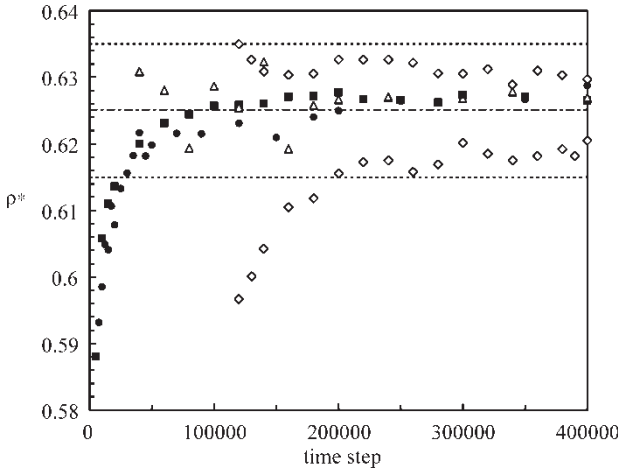

FIGURE 5 Liquid density ρ_l^* for a pure LJ fluid as a function of simulation time steps. Symbols and conditions are as in Fig. 4.

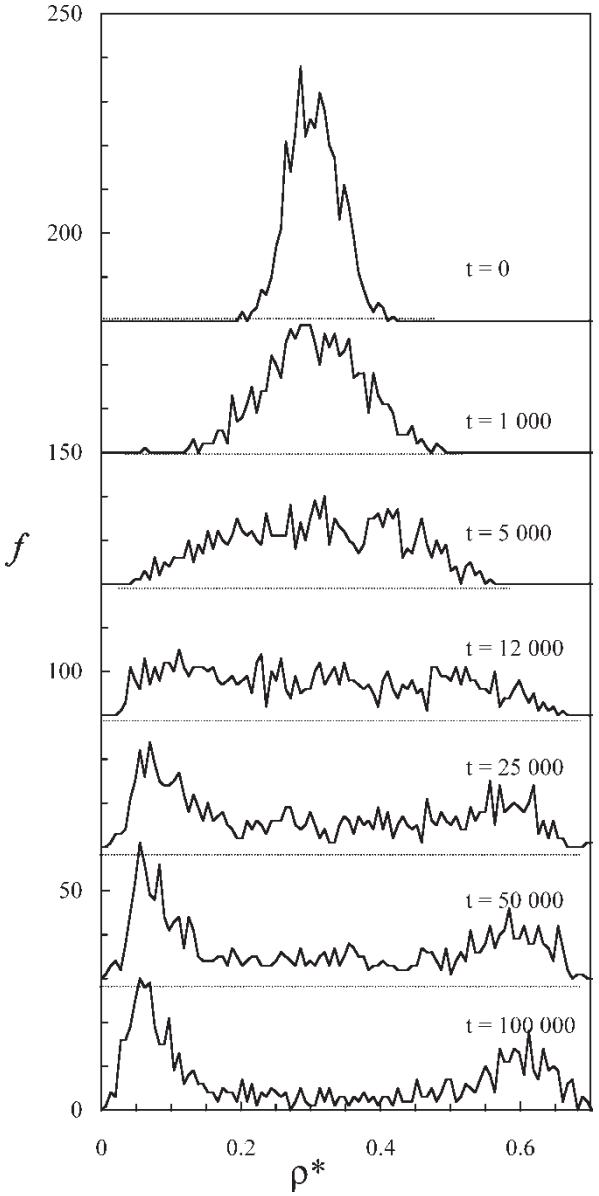

FIGURE 6 Frequency of occurrence, f, as a function of the subcell density ρ^* for a system with 30,000 LJ particles after quenching to a temperature, $T^* = 1.1$. Curves from top to bottom show the system evolution after 0, 1000, 5 000, 12,000, 25,000, 50,000 and 100,000 times steps, respectively. All curves are displaced 30 units in the vertical direction for clarity; dashed lines indicate the respective baselines. Final equilibrium vapor and liquid densities for this system correspond to 0.0655 and 0.627, respectively.

evolution of the density histograms for this system. Further evolution of the system at times longer than 100,000 time steps does not improve significantly the resolution of the histogram, pointing out that one may indeed proceed with the equilibrium property determination at this last point.

We have made a comparison with the more common application of MD simulations, namely volume expansion molecular dynamics (VEMD), in which a slab of equilibrated and reasonably high density liquid is put in contact with a slab of void space. The system is left to evolve under usual canonical MD conditions.

The apparent advantage of this set up is the *a priori* placement of a flat interface. To compare the performance of this method to TQMD, we performed VEMD simulations of two analogs of the systems studied by TQMD, namely pure LJ systems of sizes $N = 30,000$ and 500,000 particles at $T^* = 1.1$. The small system was set up at an initial density of $\rho^* = 0.814$ (box of dimensions $32 \times 32 \times 36$ in units of σ) which was expanded to a global density of $\rho^* = 0.305$ (box of dimensions $32 \times 32 \times 96$ in units of σ). The larger system was set up at an initial density of $\rho^* = 0.808$ (box of dimensions $75 \times 75 \times 110$ in units of σ) which was expanded to a global density of $\rho^* = 0.296$ (box of dimensions $75 \times 75 \times 300$ in units of σ). As a comparison, the results of the equivalent TQMD simulations shown in Figs. 4 and 5 are started as a liquid at a global density of $\rho^* = 0.305$ (30,000 particles in a box of dimensions $32 \times 32 \times 96$ in units of σ) and $\rho^* = 0.296$ (500,000 particles in a box of dimensions $75 \times 75 \times 300$ in units of σ) which is cooled down from an initial temperature of $T^* = 3$ to the final temperature of $T^* = 1.1$.

In Figs. 4 and 5, the larger VEMD system shows the "break-up" of the initial liquid slab into two domains, each of which eventually stabilize into equilibrium phases with corresponding interfaces to vapor phases. This break-up, although in principle, undesirable and not always occurring, is a natural consequence of unavoidable fluctuations in the original configuration, and the product of an explosive "boiling" of the liquid slab into the vacuum space imposed at the start of the simulation. It has been reported in previous studies in this method [8]. Figure 5 shows the time evolution of the liquid density in the systems. After 100,000 time steps, in the VEMD one can distinguish two liquid slabs being formed, and an estimate of the density may be obtained. Both domains are different in nature and have different trends towards the equilibrium result. In the VEMD simulations, the starting points are fully established liquid domains, and equilibrium must be established by liquid phase diffusion. It is seen that even after 400,000 time steps, the system is not fully equilibrated. As a comparison, the results of equivalent TQMD simulation are shown, where it is seen that the densities converge more rapidly to the expected result.

While in general the larger system sizes appear to have better statistics for a fixed number of MD time steps, the larger system size TQMD calculations also take up much more computer time than the comparable smaller ones, since in the larger systems, each individual time step involves over an order of magnitude more numerical operations. Figures 7 and 8 show the actual CPU times for the TQMD systems discussed above and compare the times with those for the corresponding GEMC calculation. Clearly, the GEMC calculations are faster in wallclock time, in spite of the parallelization of the MD codes. We make the point that the times presented correspond to a particular hardware/software combination, but do serve as a relative reference for performance.

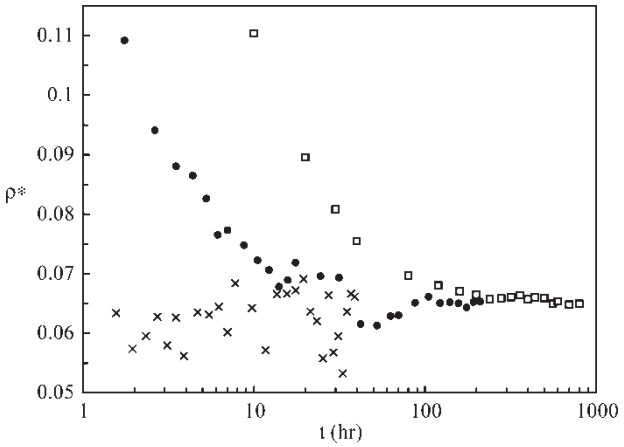

FIGURE 7 Vapor density ρ_V^* as a function of computer time for a pure LJ fluid at a temperature of $T^* = 1.1$. Crosses are GEMC results for 4000 particles. Solid circles correspond to TQMD simulations of a system of 30,000 particles, open squares correspond to a system of 500,000 particles.

Binary LLV LJ Mixture

We have studied a binary LJ system, where both components differ in size and energy. The parameters used throughout this work correspond to $\varepsilon_2/\varepsilon_1 = 0.95$, $\sigma_2/\sigma_1 = 0.8$. For the unlike-pair interactions we used binary interaction parameters large enough to force the system into a type III behavior. We used $\varepsilon_{ij} = (1 - k_{ij})\sqrt{\varepsilon_i \varepsilon_j}$ with $k_{ij} = 0.3$ and $\sigma_{ij} = 0.5(1 - l_{ij})(\sigma_i + \sigma_j)$ with $l_{ij} = 0.05$, where i and j refer to the pure component values. All thermodynamic properties are reduced with respect to component 1. Simulations were performed at a temperature $T^* = 1$ and with a CS potential at a radius of $r_{cut} = 5\sigma_1$.

The particular system studied exhibits LLE, as shown in Fig. 9. Results are calculated using 180,000

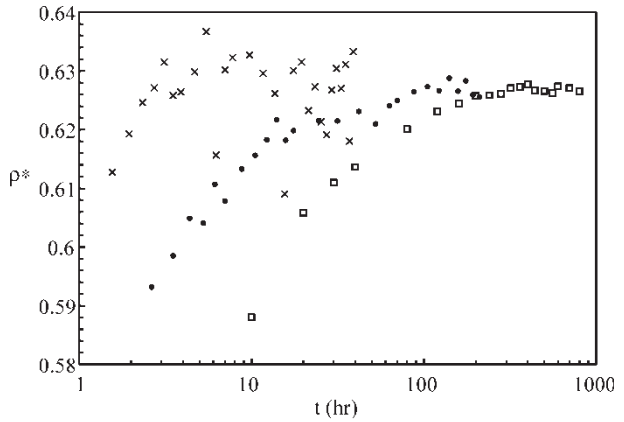

FIGURE 8 Liquid density ρ_l^* as a function of computer time. Symbols and conditions as are in Fig. 7.

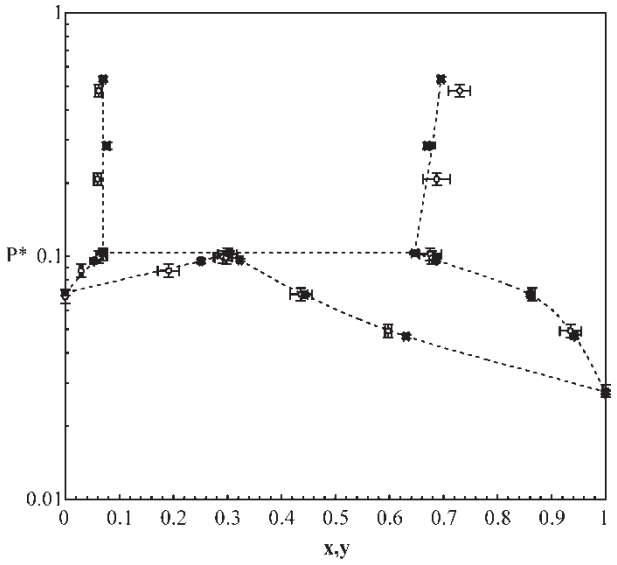

FIGURE 9 Pressure P^* composition diagram for a binary LJ mixture described in the text. Open circles are GEMC results and squares are TQMD. Data are in Table II. Lines are a guide to the eye and show the approximate phase boundaries.

particles at a temperature of $T^* = 1.0$. By varying the overall composition, different state points are obtained. The data are given in Table II. At low pressures, only VLE is present, however, as the pressure increases, a triple VLLE point is evident which delimits the LLE equilibria. The TQMD data compares favorably to the two-phase results from GEMC.

A TQMD simulation performed close to the triple point is likely to exhibit a vapor phase and a dense phase with evidence of two distinct liquid domains (c.f. Fig. 10). In spite of the uniqueness of the triple point, its appearance in a TQMD simulation is rather simple, since the "window" of densities and global compositions that satisfy the mass balance equations is rather large. On the contrary, such an exploration using GEMC requires elaborate coding. In the case of LLE, the two-box GEMC method must be performed with caution [18] since it may erroneously produce results in cases in which an additional vapor phase may be present. Examples are the simulations of Guo *et al.* [19], which for a similar system seemed to indicate a LLE with an upper critical solution temperature, which were later proven [20] to be actually VLLE and even VLE state points at the stated temperatures.

In multicomponent TQMD, the particles are initially well mixed within the whole system. Composition equilibration is driven by Fickian diffusion processes, where large concentration gradients speed up equilibration. Upon quenching, small clusters of either phase begin to form in a more or less uniform way throughout the system. At this stage, most molecules could be considered "interfacial", since domains are not yet formed. This guarantees a rather large interfacial area and a minimal diffusion path. In the case of the TQMD, compositions are equilibrated locally in fast way, mainly due to the shorter diffusion paths. These small clusters equilibrate rapidly and the system later evolves until the domains fully aggregate. Here, TQMD offers a significant advantage over VEMD where multicomponent diffusion over bulk regions must take place, a process lengthy for dense phases.

Eicosane Saturated Liquid Density

In order to illustrate another strength of the TQMD approach, the phase diagram of pure eicosane (n-C_{20}) was calculated. The intermolecular potential is a united atom (UA) representation, in which methyl and methylene groups are clustered into individual Lennard Jones spheres, connected by rigid bonds with harmonic bond bending potentials. The intra- and intermolecular potential and parameters are given in detail in Ref. [9] and used herein with no further modification. We have used a cutoff radius of 11 Å, and the parameters corresponding to that cutoff.

A random configuration of 1944 molecules was setup in a cubic cell of side 165.8 Å at a density of $0.2\,g/cm^3$ with customary periodic boundary conditions. The random configuration was initially

TABLE II VLE, LLE and VLLE pressure (P^*), density(ρ^*), molar composition of component 1 (x,y) data for a binary LJ cut and shifted ($r_c^* = 5$) potential as obtained from TQMD at $T^* = 1.0$. $\varepsilon_2/\varepsilon_1 = 0.95$, $\varepsilon_{12}/\varepsilon_1 = 0.682$, $\sigma_2/\sigma_1 = 0.8$, $\sigma_{12}/\sigma_1 = 0.855$

	Vapor		*Liquid 1*		*Liquid 2*	
P^*	ρ^*	Y	ρ^*	x	ρ^*	x
0.0276(5)	0.0332(5)	1	0.688(1)	1		
0.047(1)	0.057(1)	0.631(4)	0.701(2)	0.942(1)		
0.069(1)	0.089(1)	0.443(7)	0.723(2)	0.861(1)		
0.096(1)	0.140(1)	0.323(3)	0.758(2)	0.687(2)		
0.071(2)	0.090(2)	0			1.285(4)	0
0.095(2)	0.135(2)	0.251(2)			1.214(3)	0.053(1)
0.103(1)	0.157(1)	0.304(3)	0.787(3)	0.647(6)	1.210(6)	0.069(5)
0.28(1)			0.83(2)	0.669(5)	1.242(5)	0.077(5)
0.53(2)			0.869(6)	0.695(5)	1.302(4)	0.070(4)

0.123(4) corresponds to 0.123 ± 0.004. All properties are reduced with respect to the energy and size parameters of component 1.

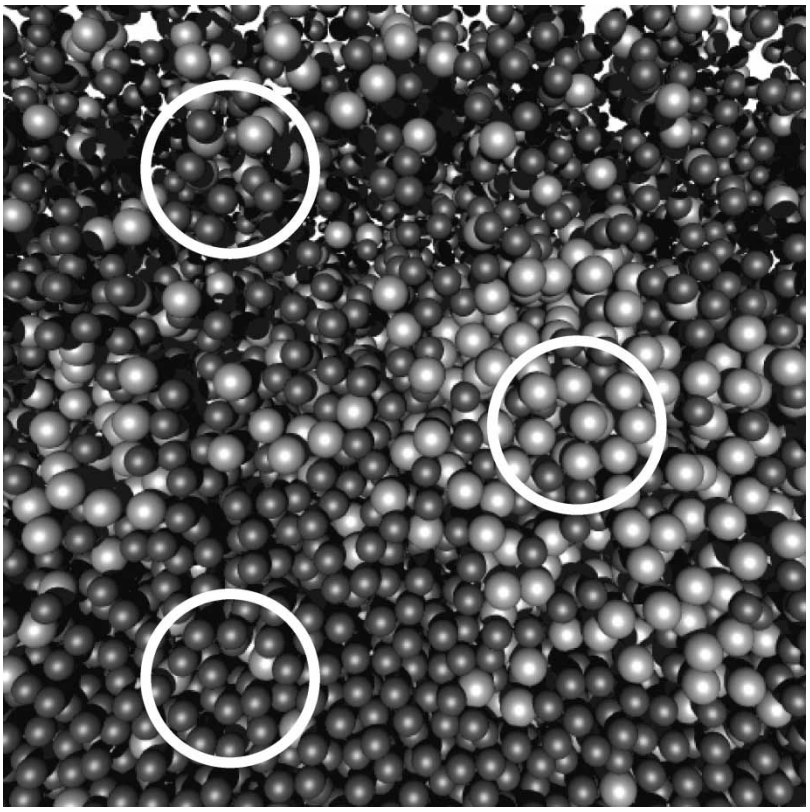

FIGURE 10 Close-up snapshot of a three-phase system, corresponding to the triple point for the binary system described in the text. Upper circle highlights a section of a vapor cluster, middle and lower circles highlight sections of two distinct liquid bulk phases, labeled liquid 1 and liquid 2, respectively in Table II.

heated up to 850 K for 200,000 time steps of 0.002 ps and was used as the starting configuration for the quenches. This configuration was quenched to the desired temperature and after 50,000 time steps of 0.005 ps, we selected five configurations at intervals of 10,000 time steps to analyze, i.e. the runs were stopped at 100,000 time steps.

In this particular case, as is also the case in oligomers and polymers, due to the elongation and repetition of the units in the molecule, the effective local density is dictated by the UA units (i.e. methyl and methylene groups which account to a total of 38,880 units) rather than by the actual placement of the center of mass or the center of the molecule. Each configuration was divided into cubic subcells of 12 Å of side for histogramming purposes. A histogram of the UA units was made and with it, the local liquid density was evaluated. Figure 11 shows an example of the analysis, where in spite of the "noise" in the histogram, three peaks are shown clearly, corresponding to the vapor, interface and liquid densities. To account for the accuracy of the procedure mentioned above, the quench at 450 K was run for 300,000 time steps until a stable flat interface was formed. An analysis of the bulk phases rendered, within experimental error, the same results obtained with TQMD. Vapor phase histogramming is subject to the problem of detecting the UA groups that form part of the interfacial regions, since due to the length of the molecule, some part of a given molecule at an interface may "point out" into the void regions, counting as groups in the vapor phase. The expected

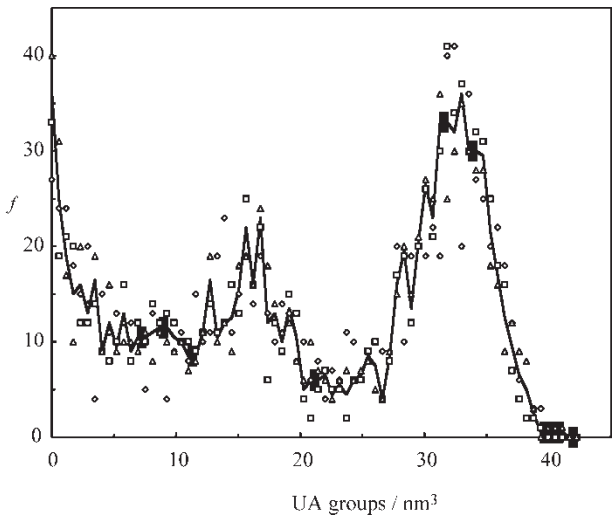

FIGURE 11 Frequency of occurrence, f, as a function of the subcell united atom (UA) group density for a system composed of 1944 eicosane ($C_{20}H_{42}$) molecules (38,880 UA groups) at 310 K. Diamonds are for the configuration at 250 ps (50,000 time steps) after the quench, squares are after 350 ps (70,000 time steps) and triangles are after 450 ps (90,000 time steps). Solid line is the average.

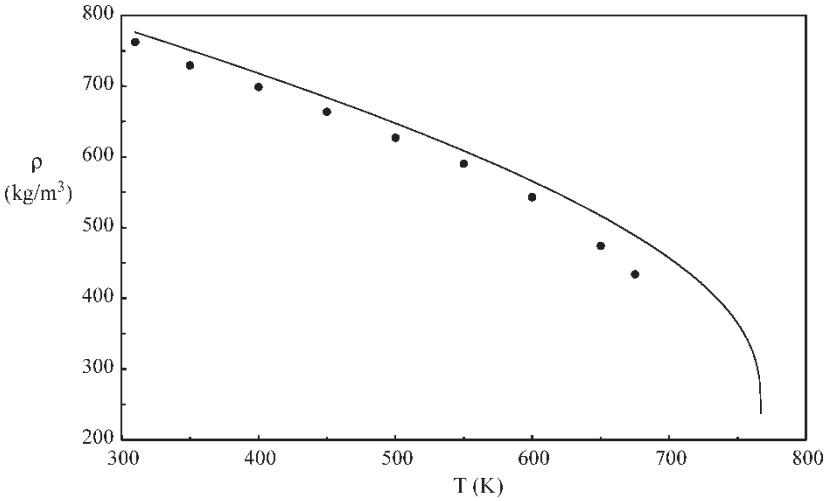

FIGURE 12 Saturated liquid density of eicosane ($C_{20}H_{42}$) as a function of temperature. Solid line is the published smoothed data [21], symbols are TQMD. Error bars are smaller than the symbol size.

low densities here suggest the need of larger system sizes or the evolution of the system towards a planar interface for further analysis if gas phase properties are to be accurately detected. For the highest temperatures probed, i.e. as the critical temperature is approached, the width of the interfacial region tends to dominate the histogram corresponding to liquid and vapor peaks, becomes more difficult to deconvolute. Here again, the evolution towards a planar interface and latter analysis via a smooth function (e.g. Ref. [9]) is a better approach than TQMD histogramming.

In Fig. 12 we plot the liquid density results along with those available from published data sources [21]. The liquid density seems consistently underestimated by the Supple and Quirke potential. It is noted that the potential was actually fit to decane and smaller alkane phase equilibria, and the use made of it here is an extrapolation. It is well known that subtle changes in the potentials may induce significant errors in the prediction of thermophysical properties. A better fit can presumably be achieved by a proper rescaling of the parameters.

CONCLUSIONS

We present a detailed analysis of the equilibration process in the TQMD method. The extremely fast quenches accessible to simulation provide a large driving force for phase separation and it is shown how, contrary to what is commonly thought, local equilibration of densities and compositions occurs quickly, and that these densities and compositions are representative of the bulk equilibrium values. If one performs the analysis of a configuration at this intermediate point, simulation times are greatly reduced, since one need not wait until the full development of a planar interface.

The results obtained by this method are shown to be of the same precision as those obtained by GEMC or VEMD. Although actual wallclock simulation times for TQMD are longer than comparable GEMC runs, TQMD can be applied in a straightforward way to more types of phase equilibrium and more complex molecular species and is especially suited for dense fluid phase equilibria, for complex molecules and for multicomponent or polydisperse systems. Furthermore, the use of MD for these calculations enables the possibility of using parallel computers. The trends of increasing availability, lower cost and simplicity of use of parallel computer setups further enhances the potential of the method.

Acknowledgements

We thank Prof Lev D. Gelb for lengthy discussions and helpful comments.

APPENDIX A: SIMULATION DETAILS

Calculations for the Lennard–Jones fluids, including the VEMD and GEMC comparisons were performed using the lj2 v16 program suite.[‡] For these MD simulations, the integration is accomplished with a 5th-order Gear predictor–corrector algorithm and temperature is controlled with the Nosé-Hoover thermostat. Time steps are fixed at $\Delta t^* = \Delta t/\sigma_1\sqrt{m/\varepsilon_1} = 0.004$, where m is an arbitrary mass of a molecule. Parallel MD simulations are set up on clustered workstations using a spatial-decomposition

[‡]http://www.chemistry.wustl.edu/~ gelb/lj2/

approach, in which a fraction of the system volume is assigned to each processor using a three-dimensional decomposition scheme [22,23]. In the case of TQMD, domain-decomposition algorithms will present by nature a load unbalance, particularly in the case of the presence of a vapor phase. Atomic decomposition or replicated data parallelization schemes, in which a given fraction of molecules (or segments) are assigned to each processor, might be a better choice for TQMD, but imposes higher overhead in communication costs [22].

Calculations for eicosane were performed using the DL_POLY program,[¶] with a replicated data parallelization algorithm.

All calculations were performed on the CAR laboratory[§] at USB. The calculations here have all been performed on a cluster of dual-processor PCs connected via a Myrinet switch. Most calculations were made using twelve "worker" processors and one "master" processor for input/output. Simulation boxes for LJ fluids were elongated threefold in one dimension (z) in order to force the formation of interfaces normal to that direction at long simulation times. This is not necessary in the TQMD scheme, and is used only for visualization purposes.

References

[1] Ladd, A.J.C. and Woodcock, L.V. (1978) "Interfacial and co-existence properties of the Lennard–Jones system at the triple point", *Mol. Phys.* **36**, 611.

[2] Holcomb, C.D., Clancy, P., Thompson, S.M. and Zollweg, J.A. (1992) "A critical study of simulations of the Lennard–Jones liquid–vapor interface", *Fluid Phase Equilibr.* **75**, 185.

[3] Holcomb, C.D., Clancy, P. and Zollweg, J.A. (1993) "A critical study of the simulation of the liquid–vapour interface of a Lennard–Jones fluid", *Mol. Phys.* **78**, 437.

[4] Panagiotopoulos, A.Z. (1987) "Direct determination of phase coexistence properties of fluids by Monte Carlo simulation in a new ensemble", *Mol. Phys.* **61**, 813. For the latest review, see Panagiotopoulos, A.Z. (2000) "Monte Carlo methods for phase equilibria of fluids" *J. Phys.-Cond. Matter*, **12**, R25.

[5] Mecke, M., Winkelmann, J. and Fischer, M. (1999) "Molecular dynamics simulation of the liquid–vapor interface: binary mixtures of Lennard–Jones fluids", *J. Chem. Phys.* **110**, 1188.

[6] Dang, L.X. (1999) "Intermolecular interactions of liquid dichloromethane and equilibrium properties of liquid–vapor and liquid–liquid interfaces: a molecular dynamics study", *J. Chem. Phys.* **110**, 10113.

[7] Nicolas, J.P. and Smit, B. (2002) "Molecular dynamics simulations of the surface tension of n-hexane, n-decane and n-hexadecane", *Mol. Phys.* **100**, 2471–2475.

[8] Pámies, J.C., McCabe, C., Cummings, P.T. and Vega, L.F. (2003) "Coexistence densities of methane and propane by canonical molecular dynamics and Gibbs Ensemble Monte Carlo simulations", *Mol. Simul.* **29**, 463.

[9] Supple, S. and Quirke, N. (2003) "Short range united atom potentials for alkanes: decane and nonane", *Mol. Simul.* **29**, 77.

[10] Gelb, L.D. and Müller, E.A. (2002) "Phase equilibria by means of temperature-quench molecular dynamics", *Fluid Phase Equilibr.* **203**, 1.

[11] Müller, E.A. and Gelb, L.D. (2003) "Molecular modeling of fluid phase equilibria using an isotropic multipolar potential", *Ind. Eng. Chem. Res.* **42**, 4123.

[12] Cahn, J.W. (1965) "Phase separation by spinodal decomposition in isotropic systems", *J. Chem. Phys.* **42**, 93.

[13] Laradji, M., Mouritsen, O.G. and Toxvaerd, S. (1996) "Spinodal decomposition in multicomponent fluid mixtures: a molecular dynamics study", *Phys. Rev. E* **53**, 3672.

[14] Gelb, L.D. and Gubbins, K.E. (1997) "Liquid–liquid phase separation in cylindrical pores; quench molecular dynamics and Monte Carlo simulations", *Phys. Rev. E* **56**, 3185.

[15] Allen, M.P. and Tildesley, D.J. (1987) *Computer Simulation of Liquids* (Oxford University Press, Oxford).

[16] Heyes, D.M. (1998) *The liquid State: Applications of Molecular Simulations* (Wiley, Chichester).

[17] Ikeshoji, T., Hafskjold, B. and Furuholt, H. (2003) "Molecular-level calculation scheme for pressure in inhomogeneous systems of flat and spherical layers", *Mol. Simul.* **29**, 101.

[18] van Leeuwen, M.E., Peters, C.J., Arons, J.D. and Panagiotopoulos, A.Z. (1991) "Investigation to the transition of liquid–liquid immiscibility for Lennard–Jones systems, using Gibbs-ensemble molecular simulations", *Fluid Phase Equilibr.* **66**, 57.

[19] Guo, M., Li, Y., Li, Z. and Lu, J. (1994) "Molecular simulation of liquid–liquid equilibria for Lennard–Jones fluids", *Fluid Phase Equilibr.* **98**, 129.

[20] Tang, Y. and Lu, B.C.-Y. (1999) "Phase equilibria study of Lennard–Jones mixtures by an analytical equation of state", *Fluid Phase Equilibr.* **165**, 183.

[21] Daubert, T.E. and Danner, R.P. (1994) *Physical and Thermodynamic Properties of Pure Chemicals*, 4th ed. (Taylor & Francis).

[22] Plimpton, S. (1995) "Fast parallel algorithms for short-range molecular dynamics", *J. Comp. Phys.* **117**, 1.

[23] Heffelfinger, G.S. (2000) "Parallel atomistic simulations", *Comp. Phys. Commun.* **128**, 219.

[¶] http://www.cse.clrc.ac.uk/msi/software/DL_POLY/

[§] http://www.car.labf.usb.ve/